

Function, Subcellular Localization and Assembly of a Novel Mutation of KCNJ2 in Andersen's Syndrome

Authors' names:

Yukio Hosaka, MD; Haruo Hanawa, MD, PhD; Takashi Washizuka, MD, PhD;
Masaomi Chinushi, MD, PhD; Fumio Yamashita, MD, PhD; Tsuyoshi Yoshida, MD;
Satoru Komura, MD; Hiroshi Watanabe, MD; Yoshifusa Aizawa, MD, PhD

Division of Cardiology, Niigata University Graduate School of Medical & Dental Sciences.

Address for Correspondence:

Yukio Hosaka, MD

Division of Cardiology, Niigata University Graduate School of Medical & Dental Sciences, Asahimachi 1-754, Niigata, 951-8510 JAPAN.

Tel: +81-25-227-2185

Fax: +81-25-227-0774

E-mail address: hosaka@med.niigata-u.ac.jp

Running head: Characteristics of a Novel Mutation of KCNJ2

Abstract

Andersen's syndrome, which is characterized by periodic paralysis, cardiac arrhythmias and dysmorphic features, is a hereditary disease, and missense mutations of KCNJ2, which encodes an inward rectifying potassium channel, have been reported recently. We performed clinical and molecular analyses of a patient with Andersen's syndrome, and found a novel mutation (G215D) of KCNJ2. Twelve lead electrocardiography revealed a long QT interval and frequent premature ventricular contractions, and polymorphic ventricular tachycardia was induced by programmed electrical stimulation. Use of a conventional whole-cell patch-clamp system with COS7 cells demonstrated that the G215D mutant was non functional, and that co-expression of wild type (WT)- and mutant-KCNJ2 shows a dominant negative effect on both inward and outward currents. We performed confocal laser scanning microscopy to assess the cellular trafficking of WT- and mutant-KCNJ2 subunits tagged with yellow fluorescent protein (YFP) and cyan fluorescent protein (CFP), respectively. Tagging with the YFP did not affect the channel function of WT-KCNJ2 and both proteins showed similar plasma membrane fluorescence patterns. Furthermore, the result of fluorescence resonance energy transfer (FRET) studies at the plasma membrane region suggested that both YFP-tagged WT- and CFP-tagged mutant-KCNJ2 combine to construct a hetero-multimer of the potassium channel. In conclusion, the G215D mutant of KCNJ2 is distributed normally in the plasma membrane, but exhibits a dominant negative effect and reduces the Kir2.1 current, presumably due to hetero-multimer construction.

Key Words

Andersen's syndrome; mutation; KCNJ2; potassium channel; long QT; ventricular tachycardia; patch-clamp; confocal laser scanning microscopy; trafficking; fluorescence resonance energy transfer (FRET)

Introduction

Clinically, Andersen's syndrome (AS) is a triad of periodic paralysis, cardiac dysrhythmias, and dysmorphic features.¹⁻⁶ Recently, Plaster et al reported 9 types of missense mutations of KCNJ2 in patients with AS.⁷ KCNJ2 encoding Kir2.1 contributes to cell excitability and resting membrane potential in excitable tissues,⁸ including the heart, brain and skeletal muscle.⁹⁻¹¹ They demonstrated that two of these nine mutations, which are expressed in *Xenopus* oocytes, have a loss of function or a strong dominant negative effect¹² on the wild type Kir2.1 channel current. Furthermore, Ai et al recently discovered a novel mutation (T192A) of KCNJ2 in a Japanese patient with familial periodic paralysis and dysrhythmias. This mutation showed a weak dominant negative effect on functional expression analysis.¹³ However, there are only a few reported cases of AS with KCNJ2 mutation, and the mechanism of the functional differences between these mutations has not been clarified.

In the present study, we report a novel missense mutation (G215D) in the intracellular C-terminal segment of KCNJ2, in a patient with AS. Functional data using a heterologous mammalian cell expression system showed a dominant negative effect on the Kir2.1 current. This missense mutation was located within the region essential for the assembly of Kir2.1.¹⁴ We then examined whether the abnormalities of cellular transport and multimerization of Kir2.1 exist using fluorescent protein-tagged techniques.

Materials and Methods

A 34-year-old female was referred to our hospital for further treatment of a cardiac arrest due to ventricular fibrillation. She exhibited dysmorphic features (short stature, scoliosis, broad forehead, low-set ears, mandibular micrognathia and clinodactyly). At 8 years of age, she had developed generalized periodic attacks of muscular weakness. Potassium levels during these attacks ranged from 4.1 to 5.2 mEq/l. Muscular weakness did not resolve with the administration of potassium or glucose. Electromyography of limb muscles revealed a myogenic pattern. Muscle biopsy was suggestive of a myopathy with tubular aggregates. She was diagnosed with periodic paralysis and oral acetazolamide was prescribed. On admission, twelve lead electrocardiography (ECG) and 24-hour ambulatory ECG revealed a long QTc and QTU interval (QTc=0.48 seconds, QTU=0.64 seconds) with a prominent U wave (Fig. 1A), and confirmed the presence of frequent ventricular extrasystoles (36620 beats/day, 38 % of daily total beat), including a non-sustained ventricular tachycardia. After obtaining written, informed consent, an electrophysiological study was performed using the standard technique.¹⁵ Polymorphic ventricular tachycardia was induced by double ventricular extrastimuli from the right ventricular outflow tract. A transvenous implantable cardioverter defibrillator system (Medtronic, Micro Jewel II 7223Cx, Minneapolis, MN) was subsequently implanted. She has a sister and a son, but her parents died in her childhood. Her sister and son lacked ECG abnormality. There was no family history of sudden cardiac death, periodic paralysis or dysmorphic features. A clinical diagnosis of AS was made by the triad of periodic paralysis, cardiac arrhythmias and dysmorphic features, as previously reported.^{2,4,6}

DNA isolation and mutational analysis

After written, informed consent was obtained for genetic analysis, genomic DNA was isolated from peripheral blood leukocytes using Sepa Gene (Sanko, Tokyo, Japan). Primers that can determine entire coding region sequences were constructed on the basis of intron and exon sequences (Table 1), and the KCNJ2 gene was amplified with each primer. PCR products were sequenced with these same primers using a BigDye Terminator Ready Reaction Mix kit (Perkin-Elmer/Applied Biosystems, Foster city, CA) and an ABI-Prism 310 DNA sequencer (Perkin-Elmer/Applied Biosystems).

Wild- and mutant-KCNJ2 construction for electrophysiological experiments

The entire coding region of Kir2.1 was amplified from the genomic DNA of the patient's leukocytes with KOD Plus DNA polymerase (TOYOBO Co. Ltd., Osaka, Japan), and primers (sense primer: 5'-CGAGAATTCATGGGCAGTGTGCGAACCAACCGC-3', anti-sense primer: 5'-GGAAGCGGCCGCTCATATCTCCGACTCTCGCCGTAA-3'). PCR products and the pCMS-EGFP vector (green fluorescent protein [GFP], Clontech, Palo Alto, CA) were digested with EcoRI/NotI, and then ligated using Ligation high (TOYOBO Co. Ltd.) to prepare wild type (WT)- or mutant-KCNJ2/pCMS-EGFP plasmid vectors. The codes of these plasmid constructs were confirmed by sequencing.

Wild- and mutant-KCNJ2 construction for confocal microscopy experiments

The entire coding region of Kir2.1 was amplified from the genomic DNA of the patient's leukocytes with KOD Plus DNA polymerase (TOYOBO Co. Ltd.), and primers (sense primer: 5'-CGAGAATTCATGGGCAGTGTGCGAACCAACCGC-3', anti-sense primer: 5'-TACCGTCGACTGTATCTCCGACTCTCGCCGTAA-3'). PCR products, the pEYFP-N1 vector (yellow fluorescent protein [YFP], Clontech), and the pECFP-N1 vector (cyan fluorescent protein [CFP], Clontech) were digested with EcoRI/SalI, and then ligated using the Ligation high (TOYOBO Co. Ltd.) to prepare WT-KCNJ2/pEYFP-N1 and mutant-KCNJ2/pECFP-N1 plasmid vectors. The C-termini of WT- and mutant-KCNJ2 were tagged with YFP and CFP. The codes of these plasmid constructs were confirmed by sequencing.

Transfection and cell culture

COS7 cells were seeded at a density of 1.5×10^4 cells per 35 mm Petri dish, and cultured for 12-24 hours prior to transfection in Dulbecco's modified Eagle's medium (Invitrogen Corp., Carlsbad, CA) supplemented with 10 % fetal bovine serum (ICN Biomedicals, Inc., Aurora, OH). The cells were transiently transfected using the Lipofectamine method (Invitrogen Corp.). In the electrophysiological experiments, 2 μg or 1 μg of WT-KCNJ2/pCMS-EGFP, 1 μg of WT- and 1 μg of mutant-KCNJ2/pCMS-EGFP, or 2 μg of mutant-KCNJ2/pCMS-EGFP were used. Transfected cells were visualized by fluorescence in the studies of expression. In confocal microscopy, 2 μg of WT-KCNJ2/pEYFP-N1, 2 μg of mutant-KCNJ2/pECFP-N1, 1 μg of WT-KCNJ2/pEYFP-N1 and 1 μg of mutant-KCNJ2/pECFP-N1, 1 μg of mutant-KCNJ2/pECFP-N1 and 1 μg of

pEYFP-Mem (YFP expressing at the plasma membrane, Clontech),¹⁶ or 2 μg of pEYFP-Mem were used.

Electrophysiological experiments

Whole-cell currents were recorded using an Axopatch 200B amplifier (Axon Instruments, Foster city, CA) 24-48 hours after transfection.¹⁷ The cells used in the electrophysiological experiments were identified by GFP fluorescence using fluorescence microscopy on the stage of an inverted microscope (OLYMPUS Optical Corp., TOKYO, Japan). All experiments were performed at 36 °C. The resistance of the pipette ranged from 5 to 10 M Ω when filled with the internal solutions of potassium aspartate, 60, KCl, 65, KH_2PO_4 , 1, MgCl_2 , 2, EDTA, 3, K_2ATP , 3, and HEPES, 5 (mM) adjusted to pH 7.4 using KOH. The bath solution contained NaCl, 140, KCl, 5.4, MgCl_2 , 0.5, CaCl_2 , 1.8, NaH_2PO_4 , 0.33, glucose, 5.5 and HEPES, 5 (mM) adjusted to pH 7.4 using NaOH. All data were digitized using a Digidata 1200 (Axon Instruments) at a sampling frequency of 2 kHz through a 1 kHz Bessel type filter (24 dB/octave, model FV664, NF Circuit, Tokyo, Japan).¹⁸ Membrane currents were usually elicited by 150 msec pulses applied in 10 mV increments, to potentials ranging from -140 to 0 mV, from a holding potential of -80 mV. Data analysis was performed using a pClamp 6 (Axon Instruments) and ORIGIN 6.1 software (Microcal Inc., Northampton, MA). The steady-state currents were measured, and current density (pA/pF) was calculated by dividing with each membrane capacitance, and is described in the text, unless otherwise mentioned.

Confocal microscopy experiments

WT-KCNJ2/pEYFP-N1, mutant-KCNJ2/pECFP-N1, or pEYFP-Mem plasmid vectors were transfected to COS7 cells in glass bottomed microwell dishes. Forty-eight hours after transfection, cells were imaged using confocal microscopy. Confocal microscopy was performed with a Fluoview FV500 confocal laser scanning microscope (version 4.0, OLYMPUS Optical Corp.). In some experiments, transfected COS7 cells were chemically stripped from the glass bottomed microwell dish by treatment with 0.25 % trypsin for 60 seconds, to minimize the cell surface.¹⁹ A multi argon laser (excitation wavelength=515 nm) was used to excite the YFP, and a multi argon laser (excitation wavelength=458 nm) was used to excite the CFP. YFP fluorescence was detected with the BP535/565 filter set and assigned as yellow. CFP fluorescence was detected with the BP465/495 filter set and assigned as blue. Two-color images were obtained by overlaying images from individual channels using the Fluoview FV500 confocal laser scanning microscope. To clarify if fluorescence resonance energy transfer (FRET) between an excited fluorescent donor (mutant-KCNJ2/pECFP-N1) and an acceptor (WT-KCNJ2/pEYFP-N1 or pEYFP-Mem) occurs in the co-expression of mutant-KCNJ2/pECFP-N1 and WT-KCNJ2/pEYFP-N1, or mutant-KCNJ2/pECFP-N1 and pEYFP-Mem, we performed photobleaching of the YFP, using a high intensity exposure to the YFP excitation light for 30 seconds. When CFP and YFP exhibit FRET, photobleaching of the YFP leads to an increase in CFP emission. To confirm that both WT-KCNJ2/pEYFP-N1 and mutant-KCNJ2/pECFP-N1 are located close in the plasma membrane, we analyzed the fluorescence signal from only the plasma membrane region. The ratio was calculated by dividing the CFP and YFP emission intensity after

photobleaching by the emission intensity before photobleaching.²⁰⁻²² Digitized image data obtained from the experiment were prepared for presentation using Photoshop 6.0 (Adobe systems, Mountain View, CA).

Statistical analysis

All numerical values were expressed as mean±S.E.M. (number of observations). For electrophysiological experiments, the statistical analysis was performed using ANOVA and Bonferroni test, with $p < 0.0167$ considered significant. For confocal microscopy, the statistical analysis was performed using the unpaired Student's t-test, with $p < 0.05$ considered significant.

Results

Mutation analysis

DNA sequencing identified a heterozygous single nucleotide substitution in KCNJ2 at position 644 (G to A), resulting in an amino acid substitution of aspartic acid for glycine at codon 215 (G215D) (Fig. 1B). This heterozygous mutation was located in the C-terminal domain of KCNJ2. This nucleotide substitution was not observed in 100 normal individuals (data not shown). We also examined her sister and son, and no mutation was identified. Direct sequencing of other primer sets of KCNJ2 from this patient revealed no mutation. G215 is a highly conserved amino acid residue in the inward rectifying potassium channel family (Fig. 1C).

Regarding the topology of the Kir2.1 channel, G215D is located in the proximal site of the C-terminus, which is the region essential for the assembly of Kir2.1,¹⁴ and is near R218W that shows a dominant negative effect on the wild type Kir2.1 current.⁷

Functional expression of WT- and G215D mutant-KCNJ2 in COS7 cells

To investigate the effects of the G215D mutation on channel function, conventional whole-cell patch-clamp experiments were conducted on cells transfected with WT- and/or G215D mutant-KCNJ2, using a heterologous mammalian cell expression system (COS7 cells). The cells transfected with 2 μ g of mutant-KCNJ2/pCMS-EGFP alone failed to form functional homo-multimeric channels (Fig. 2A, B: G215D 2 μ g). The inward and outward current densities in the cells transfected with 1 μ g of WT-KCNJ2/pCMS-EGFP (-140 mV; -115 ± 10 pA/pF, -40 mV; 30 ± 8 pA/pF) (Fig. 2:

WT 1 μg) were smaller than those in the cells transfected with 2 μg of WT-KCNJ2/pCMS-EGFP (-140 mV ; $-192\pm 36\text{ pA/pF}$, -40 mV ; $32\pm 10\text{ pA/pF}$) (Fig. 2: WT 2 μg). The inward and outward current densities in the cells co-transfected with WT- and mutant-KCNJ2/pCMS-EGFP (-140 mV ; $-65\pm 6\text{ pA/pF}$, -40 mV ; $3\pm 2\text{ pA/pF}$) (1 μg each, Fig. 2: WT 1 μg + G215D 1 μg) were significantly lower than those in the cells transfected with 2 μg of WT-KCNJ2/pCMS-EGFP (-140 mV ; $p=0.0002$, -40 mV ; $p=0.0056$) (Fig. 2: WT 2 μg), but there was no significant difference of the reversal potential between the cells transfected with 2 μg of WT-KCNJ2/pCMS-EGFP ($-73\pm 2\text{ mV}$) and those co-transfected with WT- and mutant-KCNJ2/pCMS-EGFP (1 μg each, $-72\pm 3\text{ mV}$). Current densities of -140 mV and -40 mV were obtained in multiple cells under different conditions, and are summarized in Figure 2C as bar graphs. To compare the inward rectifying property between WT and co-transfected cells, the ratio was calculated by dividing the current density amplitudes of -40 mV by those of -140 mV . The ratio (0.044 ± 0.024) of the cells co-transfected with WT- and mutant-KCNJ2/pCMS-EGFP (1 μg each) was smaller than that (0.17 ± 0.019) of those transfected with 2 μg of WT-KCNJ2/pCMS-EGFP ($p=0.0004$). These findings demonstrated that G215D subunits exhibit a dominant negative effect on the WT Kir2.1 channel current, and accentuate the inward rectifying property.

Subcellular localization of WT- and G215D mutant-KCNJ2 in COS7 cells

To assess the cellular transport of WT- and G215D mutant-KCNJ2 in COS7 cells, we examined the subcellular localization using WT-KCNJ2/pEYFP-N1 and mutant-KCNJ2/pECFP-N1 (Fig. 3). The cells transfected with WT-KCNJ2/pEYFP-N1

showed a plasma membrane fluorescence pattern (Fig. 3A), with mutant-KCNJ2/pECFP-N1 showing a similar fluorescence pattern (Fig. 3B). In this procedure, 41 of 50 cells transfected with WT-KCNJ2/pEYFP-N1 exhibited enhanced fluorescence signals in the plasma membrane, and 38 of 50 cells transfected with mutant-KCNJ2/pECFP-N1 showed similar fluorescence patterns. Trypsinization immediately prior to a confocal microscopic analysis clearly demonstrated these findings in protein localization (Fig. 3C, 3D). The cells co-transfected with WT-KCNJ2/pEYFP-N1 and mutant-KCNJ2/pECFP-N1 were located in nearly the same region. Tagging with the fluorescent protein did not affect WT Kir2.1 channel function, because a similar conductance was consistently observed in the cells transfected with WT-KCNJ2/pEYFP-N1 (data not shown).

FRET between WT- and G215D mutant-KCNJ2 at the plasma membrane region of COS7 cells

To confirm if WT- and G215D mutant-KCNJ2 construct hetero-multimers of Kir2.1 channels in the plasma membrane, we conducted FRET studies between WT-KCNJ2/pEYFP-N1 and mutant-KCNJ2/pECFP-N1, and compared the results with those between pEYFP-Mem and mutant-KCNJ2/pECFP-N1 (Fig. 4A, B). The ratio of the CFP emission intensity (1.081 ± 0.021) of the combination of WT-KCNJ2/pEYFP-N1 and mutant-KCNJ2/pECFP-N1 was larger than that (0.99 ± 0.011) of the combination of pEYFP-Mem and mutant-KCNJ2/pECFP-N1 ($p=0.0046$) (Fig. 4C). Following photobleaching of the YFP, the CFP emission signal of only the combination of WT-KCNJ2/pEYFP-N1 and mutant-KCNJ2/pECFP-N1 increased. These findings

demonstrate that FRET is detected between WT-KCNJ2/pEYFP-N1 and mutant-KCNJ2/pECFP-N1, implying that WT-KCNJ2 and G215D mutant-KCNJ2 exist within 10 nm of each other. Thus WT and mutant subunits could combine to construct a hetero-multimer.

Discussion

We discovered a novel KCNJ2 mutation, G215D that causes the phenotype of AS, including cardiac arrhythmias, periodic paralysis and dysmorphic features. This mutation shows a dominant negative effect¹² on the WT Kir2.1 channel current, and accentuates the inward rectifying property. Kir2.1 was detected predominantly in the heart, forebrain and skeletal muscle.⁹⁻¹¹ In this patient, ECG revealed prolonged QT interval and frequent ventricular extrasystoles, as previously reported in other patients with AS.^{1-6,13}

The cells transfected with G215D mutant-KCNJ2 alone did not form functional channel. In previous studies, functional analyses were performed on three mutant subunits, D71V, R218W and T192A.^{7,13} None of these homo-multimeric channels displayed functional channels. In the functional analyses of cells co-expressing WT- and mutant-KCNJ2, the reduction in current was approximately 1/16 for D71V, 1/4 for R218W, 1/2 for T192A and 1/3 for G215D, compared with WT. The mechanism of the functional difference among these mutations has not been clarified. The dysmorphic features were lacking in the case of T192A mutant. This might depend on the extent of the reduction of Kir2.1 channel function. In several inherited diseases, deficient protein trafficking of the mutation to the plasma membrane has been reported.²³⁻²⁶ Furthermore, the proximal C-terminus, which is where G215D is located, is responsible for the assembly of Kir2.1.¹⁴ To assess these possibilities in regard to G215D, we investigated the subcellular localization and assembly of the G215D mutant-KCNJ2 using confocal microscopic images. Our study revealed that WT-KCNJ2/pEYFP-N1 and mutant-KCNJ2/pECFP-N1 show similar fluorescence patterns along the plasma membrane, and that the reduction of Kir2.1 function is not related to abnormal protein

trafficking. Furthermore, we confirmed that FRET between WT-KCNJ2/pEYFP-N1 and mutant-KCNJ2/pECFP-N1 occurs in the plasma membrane region. If excited fluorescent donor and acceptor proteins are less than 10 nm apart and are orientated appropriately, FRET may occur.^{20-22,27} To confirm that these results were not artifacts caused by the change of cell size and direct excitation of YFP by the CFP excitation laser, FRET studies between pEYFP-Mem and mutant-KCNJ2/pECFP-N1 were performed. We demonstrated that nonspecific overcrowding of proteins did not induce FRET. The data revealed that WT- and mutant-KCNJ2 exist within 10 nm in the plasma membrane region, and should be present as a hetero-multimer in the plasma membrane. The reduction of Kir2.1 function should be not related to abnormal assembly. Soom et al reported that inwardly rectifying potassium channels require the binding of phosphatidylinositol-4, 5-bisphosphate (PIP₂) for channel activity, and that three independent sites (aa 175-206, aa 207-246, aa 324-365) are located in the C-terminal domain of the Kir2.1 channels.²⁸ As G215D mutation exists in the PIP₂ binding domain (residues 207-246), it is possible that G215D mutant exhibits abnormal PIP₂ binding, and hetero-multimerization of WT and G215D mutant causes a dominant negative effect. Moreover, this mutation showed the accentuated inward rectifying property. Kubo et al reported that the negative charges of E224 and E299 contribute to inward rectifying property.²⁹ They also suggested the possibility that these two sites contribute to the inner vestibule of the Kir2.1 channel pore. The changes of blocking and unblocking processes by mutation of these sites weaken the entry of spermine to the blocking site. In this study, the negative charge of D215 might contribute to accentuate the inward rectifying property.

In conclusions, the G215D mutation, a result of G644A transition, in KCNJ2 exhibits a dominant negative effect on Kir2.1 channel function, and accentuates the inward rectifying property. Cells co-transfected with WT-KCNJ2/pEYFP-N1 and mutant-KCNJ2/pECFP-N1, were identified at the same location including in the plasma membrane region, and demonstrated that WT- and G215D mutant-KCNJ2 could construct a hetero-multimer in the plasma membrane. Assembly between WT- and G215D mutant-KCNJ2 must be the cause of the dominant negative effect. Moreover, the negative charge of D215 might accentuate the inward rectifying property.

Acknowledgments

We thank Dr. A. Kakita and Dr. H. Oshima for their kind support in the confocal microscopy experiments, and Dr. M. Matsuda and Dr. M. Igarashi for their kind support in the FRET studies. This work was partially supported by a grant for Promotion of Niigata University Research Projects.

References

1. Andersen ED, Krasilnikoff PA, Overvad H. Intermittent muscular weakness, extrasystoles, and multiple developmental anomalies. A new syndrome? *Acta Paediatr Scand* 1971; 60: 559-564.
2. Canun S, Perez N, Beirana LG. Andersen syndrome autosomal dominant in three generations. *Am J Med Genet* 1999; 85: 147-156.
3. Klein R, Ganelin R, Marks JF. Periodic paralysis with cardiac arrhythmia. *J Pediatr* 1963; 62: 371-385.
4. Sansone V, Griggs RC, Meola G, Ptacek LJ, Barohn R, Iannaccone S, Bryan W, Baker N, Janas SJ, Scott W, Ririe D, Tawil R. Andersen's syndrome: a distinct periodic paralysis. *Ann Neurol* 1997; 42: 305-312.
5. Stubbs WA. Bidirectional ventricular tachycardia in familial hypokalaemic periodic paralysis. *Proc R Soc Med* 1976; 69: 223-224.
6. Tawil R, Ptacek LJ, Pavlakis SG, DeVivo DC, Penn AS, Ozdemir C, Griggs RC. Andersen's syndrome: potassium-sensitive periodic paralysis, ventricular ectopy, and dysmorphic features. *Ann Neurol* 1994; 35: 326-330.

7. Plaster NM, Tawil R, Tristani-Firouzi M, Canun S, Bendahhou S, Tsunoda A, Donaldson MR, Iannaccone ST, Brunt E, Barohn R, Clark J, Deymeer F, George AL, Jr., Fish FA, Hahn A, Nitu A, Ozdemir C, Serdaroglu P, Subramony SH, Wolfe G, Fu YH, Ptacek LJ. Mutations in Kir2.1 cause the developmental and episodic electrical phenotypes of Andersen's syndrome. *Cell* 2001; 105: 511-519.
8. Nichols CG, Lopatin AN. Inward rectifier potassium channels. *Annu Rev Physiol* 1997; 59: 171-191.
9. Isomoto S, Kondo C, Kurachi Y. Inwardly rectifying potassium channels: their molecular heterogeneity and function. *Jpn J Physiol* 1997; 47: 11-39.
10. Kubo Y, Baldwin TJ, Jan YN, Jan LY. Primary structure and functional expression of a mouse inward rectifier potassium channel. *Nature* 1993; 362: 127-133.
11. Raab-Graham KF, Radeke CM, Vandenberg CA. Molecular cloning and expression of a human heart inward rectifier potassium channel. *Neuroreport* 1994; 5: 2501-2505.
12. Herskowitz I. Functional inactivation of genes by dominant negative mutations. *Nature* 1987; 329: 219-222.
13. Ai T, Fujiwara Y, Tsuji K, Otani H, Nakano S, Kubo Y, Horie M. Novel KCNJ2

mutation in familial periodic paralysis with ventricular dysrhythmia. *Circulation* 2002; 105: 2592-2594.

14. Tinker A, Jan YN, Jan LY. Regions responsible for the assembly of inwardly rectifying potassium channels. *Cell* 1996; 87: 857-868.

15. Aizawa Y, Niwano S, Chinushi M, Tamura M, Kusano Y, Miyajima T, Kitazawa H, Shibata A. Incidence and mechanism of interruption of reentrant ventricular tachycardia with rapid ventricular pacing. *Circulation* 1992; 85: 589-595.

16. Moriyoshi K, Richards LJ, Akazawa C, O'Leary DD, Nakanishi S. Labeling neural cells using adenoviral gene transfer of membrane-targeted GFP. *Neuron* 1996; 16: 255-260.

17. Hamill OP, Marty A, Neher E, Sakmann B, Sigworth FJ. Improved patch-clamp techniques for high-resolution current recording from cells and cell-free membrane patches. *Pflugers Arch* 1981; 391: 85-100.

18. Washizuka T, Horie M, Obayashi K, Sasayama S. Genistein inhibits slow component delayed-rectifier K currents via a tyrosine kinase-independent pathway. *J Mol Cell Cardiol* 1998; 30: 2577-2590.

19. Makhina EN, Nichols CG. Independent trafficking of KATP channel subunits to the plasma membrane. *J Biol Chem* 1998; 273: 3369-3374.
20. Miyawaki A, Tsien RY. Monitoring protein conformations and interactions by fluorescence resonance energy transfer between mutants of green fluorescent protein. *Methods Enzymol* 2000; 327: 472-500.
21. Pollok BA, Heim R. Using GFP in FRET-based applications. *Trends Cell Biol* 1999; 9: 57-60.
22. Wilson MC, Meredith D, Halestrap AP. Fluorescence resonance energy transfer studies on the interaction between the lactate transporter MCT1 and CD147 provide information on the topology and stoichiometry of the complex in situ. *J Biol Chem* 2002; 277: 3666-3672.
23. Yamashita F, Horie M, Kubota T, Yoshida H, Yumoto Y, Kobori A, Ninomiya T, Kono Y, Haruna T, Tsuji K, Washizuka T, Takano M, Otani H, Sasayama S, Aizawa Y. Characterization and subcellular localization of KCNQ1 with a heterozygous mutation in the C terminus. *J Mol Cell Cardiol* 2001; 33: 197-207.
24. Ficker E, Dennis AT, Obejero-Paz CA, Castaldo P, Taglialatela M, Brown AM.

Retention in the endoplasmic reticulum as a mechanism of dominant-negative current suppression in human long QT syndrome. *J Mol Cell Cardiol* 2000; 32: 2327-2337.

25. Zhou Z, Gong Q, January CT. Correction of defective protein trafficking of a mutant HERG potassium channel in human long QT syndrome. Pharmacological and temperature effects. *J Biol Chem* 1999; 274: 31123-31126.

26. Furutani M, Trudeau MC, Hagiwara N, Seki A, Gong Q, Zhou Z, Imamura S, Nagashima H, Kasanuki H, Takao A, Momma K, January CT, Robertson GA, Matsuoka R. Novel mechanism associated with an inherited cardiac arrhythmia: defective protein trafficking by the mutant HERG (G601S) potassium channel. *Circulation* 1999; 99: 2290-2294.

27. Mochizuki N, Yamashita S, Kurokawa K, Ohba Y, Nagai T, Miyawaki A, Matsuda M. Spatio-temporal images of growth-factor-induced activation of Ras and Rap1. *Nature* 2001; 411: 1065-1068.

28. Soom M, Schonherr R, Kubo Y, Kirsch C, Klinger R, Heinemann SH. Multiple PIP2 binding sites in Kir2.1 inwardly rectifying potassium channels. *FEBS Lett* 2001; 490: 49-53.

29. Kubo Y, Murata Y. Control of rectification and permeation by two distinct sites after the second transmembrane region in Kir2.1 K⁺ channel. *J Physiol* 2001; 531.3: 645-660.

Figure Legends

Figure 1.

Heterozygous mutation of KCNJ2 in an Andersen's syndrome patient. A, ECG of the patient. B, Electropherogram of the sequence around the heterozygous mutation (G215D) of KCNJ2. C, Amino acid alignment of the Kir family around the mutation (G215D).

Figure 2.

Functional expression of WT- and G215D mutant-KCNJ2. A, Representative current traces of WT- and G215D mutant-KCNJ2 in COS7 cells. Cells of each panel were transfected as follows: WT 2 μ g; 2 μ g of WT-KCNJ2/pCMS-EGFP, WT 1 μ g; 1 μ g of WT-KCNJ2/pCMS-EGFP, WT 1 μ g + G215D 1 μ g; 1 μ g of WT- and 1 μ g of mutant-KCNJ2/pCMS-EGFP, G215D 2 μ g; 2 μ g of mutant-KCNJ2/pCMS-EGFP. B, Current-voltage relationship measured from cells transfected with WT- or G215D mutant-KCNJ2. C, Summary bar graphs of inward and outward current densities at -140 mV and -40 mV, respectively, for WT 1 μ g + G215D 1 μ g, 1 μ g or 2 μ g of WT.

Figure 3.

Subcellular localization of WT- and G215D mutant-KCNJ2 in COS7 cells. Confocal microscopic images of COS7 cells transfected with WT-KCNJ2/pEYFP-N1 (A) and

mutant-KCNJ2/pECFP-N1 (B). The cells, transfected with WT-KCNJ2/pEYFP-N1 (C) and mutant-KCNJ2/pECFP-N1 (D), were treated with trypsin.

Figure 4.

FRET using photobleaching. Cells were co-transfected with mutant-KCNJ2/pECFP-N1 and WT-KCNJ2/pEYFP-N1 (A), and mutant-KCNJ2/pECFP-N1 and pEYFP-Mem (B). Images were obtained before and after photobleaching of YFP, with bar graphs of the ratio (C: upper; CFP, lower; YFP, left; mutant-KCNJ2/pECFP-N1 and WT-KCNJ2/pEYFP-N1, right; mutant-KCNJ2/pECFP-N1 and pEYFP-Mem).

Table 1. Primers Used to Amplify KCNJ2

Primer	Forward	Reverse
1	5' GAACATTCAAAACTGTTTCTCCAA 3'	5' AGAGCTATCAACCAAAACACACAG 3'
2	5' GTGGATGCTGGTTATCTTCTGC 3'	5' GCATTGTGACTGAAGACAAGAGTC 3'
3	5' CATCATCGATGCTTTCATCATT 3'	5' ATTTCAAAGTCTGCGTTGTCAAT 3'
4	5' CCATGAAATAGATGAAGACAGTCC 3'	5' CTAGTGCTTTCTGGAACTCCATTT 3'
5	5' CTATGAAAATGAAGTTGCCCTCAC 3'	5' TGGAGACATGGTTAGTGCTTTATG 3'

The KCNJ2 gene was amplified with each primer according to the following amplification profile: 35 cycles at 94 °C for 60 seconds, 60 °C for 90 seconds, with a 120 second extension at 73 °C.

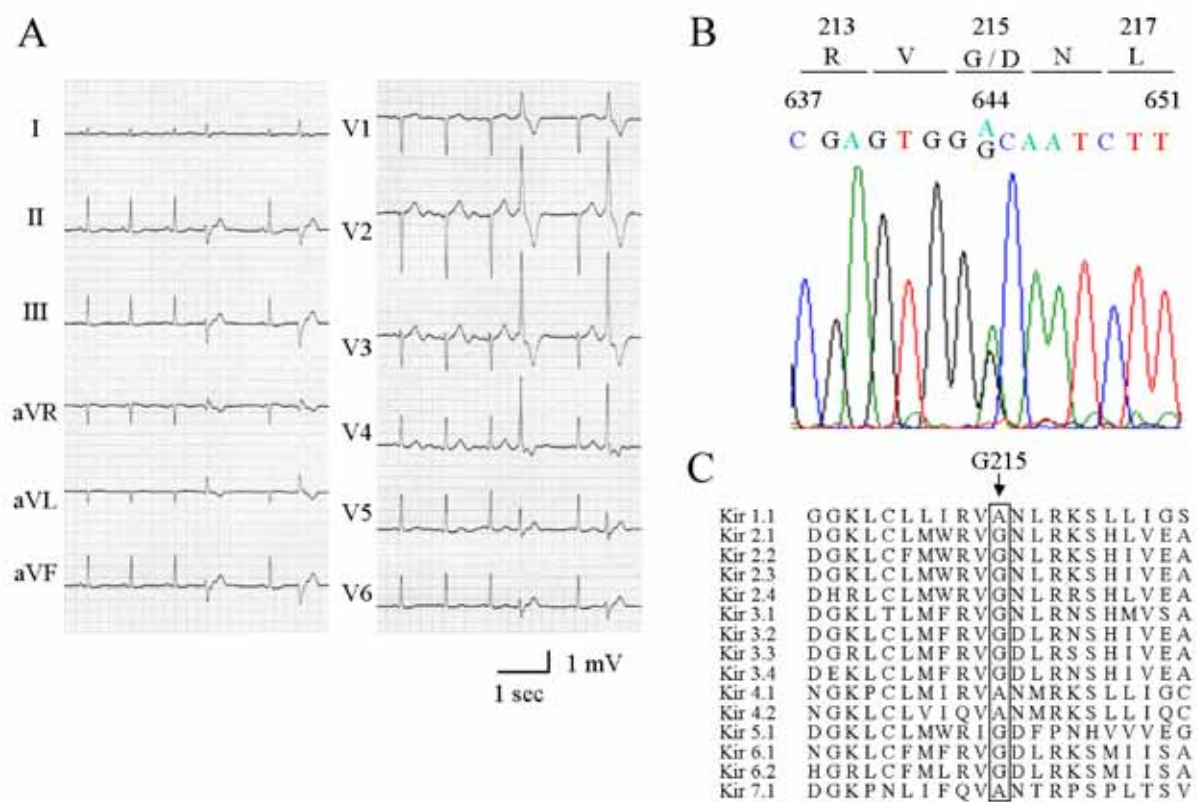
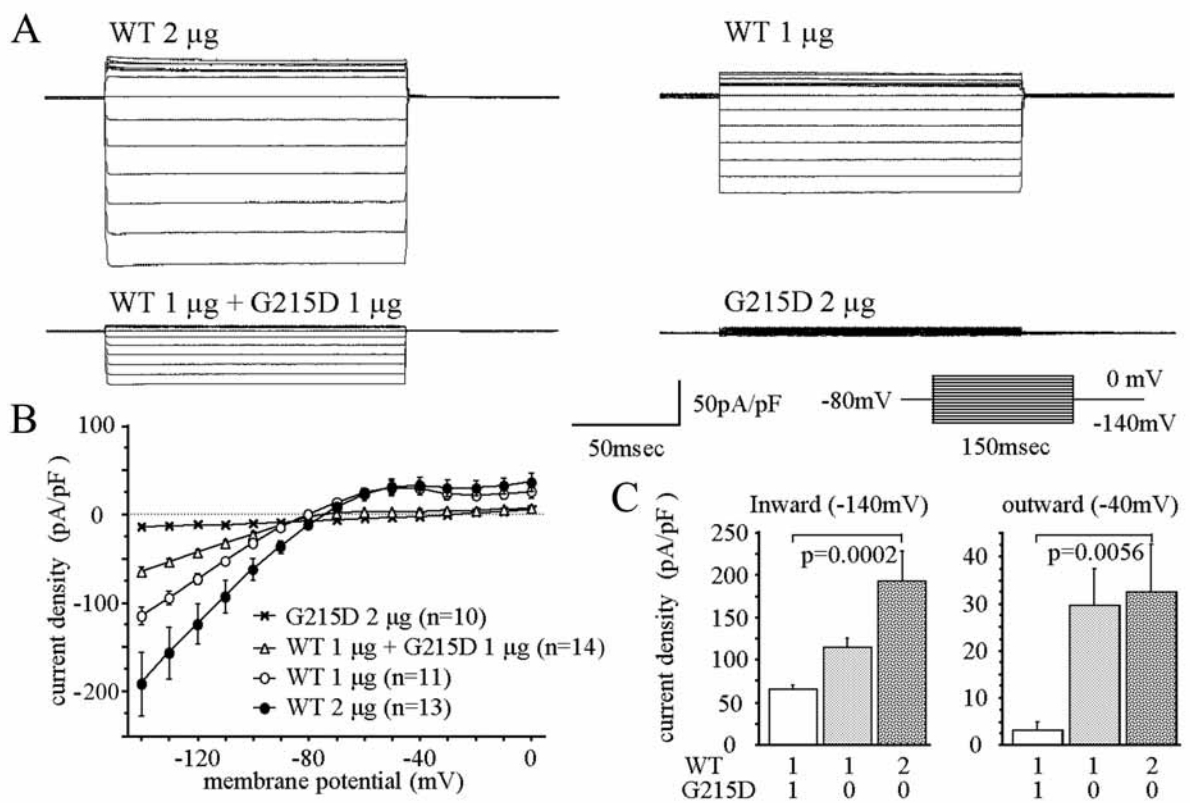


Figure 1



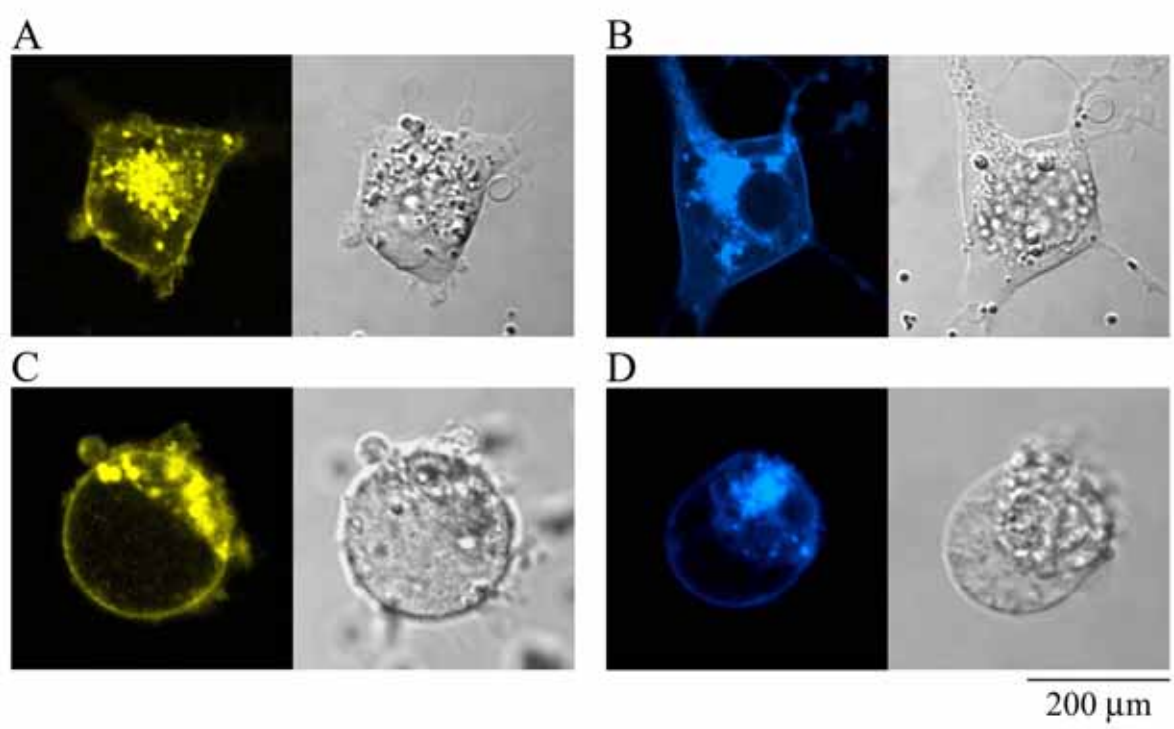


Figure 3

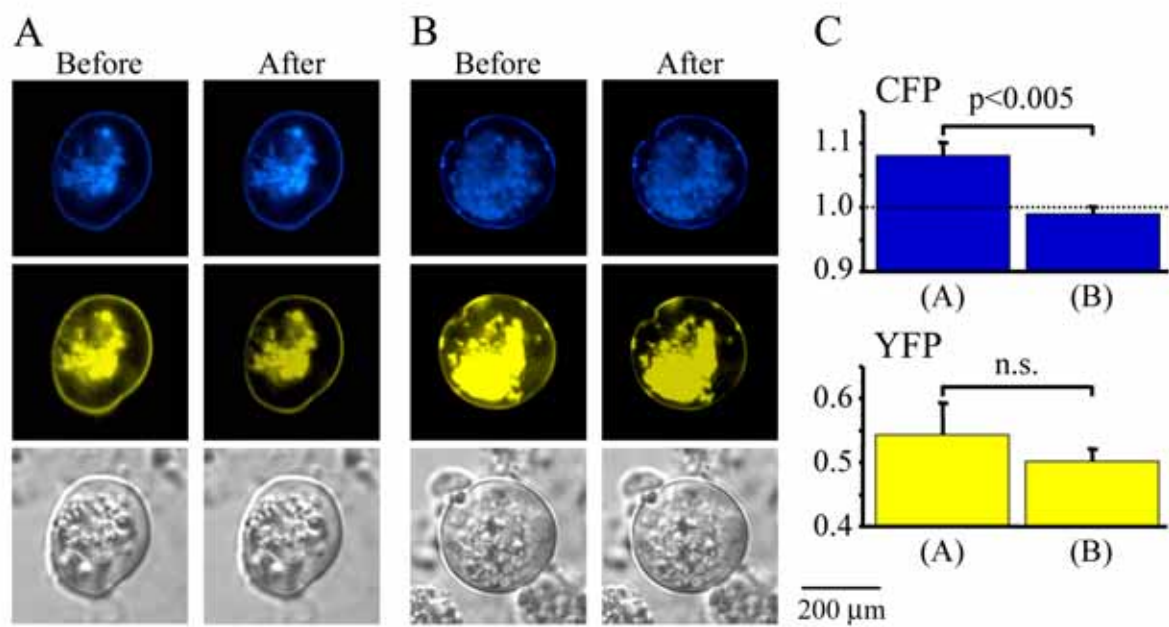


Figure 4